Journal of Electroanalytical Chemistry 639 (2010) 102–108

Contents lists available at ScienceDirect

Journal of Electroanalytical Chemistry

journal homepage: www.elsevier.com/locate/jelechem

Oxygen reduction by decamethylferrocene at liquid/liquid interfaces catalyzed by dodecylaniline

Bin Su [a,1], Imren Hatay [a,b], Fei Li [a], Raheleh Partovi-Nia [a], Manuel A. Méndez [a], Zdenek Samec [c], Mustafa Ersoz [b], Hubert H. Girault [a,*]

[a] Laboratoire d'Electrochimie Physique et Analytique, Ecole Polytechnique Fédérale de Lausanne, Station 6, CH-1015 Lausanne, Switzerland
[b] Department of Chemistry, Selcuk University, 42031 Konya, Turkey
[c] J. Heyrovsky Institute of Physical Chemistry of ASCR, v.v.i, Dolejskova 3, 182 23 Prague 8, Czech Republic

ARTICLE INFO

Article history:
Received 26 August 2009
Received in revised form 2 November 2009
Accepted 30 November 2009
Available online 10 December 2009

Keywords:
Oxygen reduction
Proton reduction
Decamethylferrocene
Liquid/liquid interface
Voltammetry

ABSTRACT

Molecular oxygen (O_2) reduction by decamethylferrocene (DMFc) was investigated at a polarized water/1,2-dichloroethane (DCE) interface. Electrochemical results point to a mechanism similar to the *EC* type reaction at the conventional electrode/solution interface, in which an assisted proton transfer (*APT*) by DMFc across the water/DCE interface via the formation of $DMFcH^+$ corresponds to the electrochemical step and O_2 reduction to hydrogen peroxide (H_2O_2) represents the chemical step. The proton transfer step can also be driven using lipophilic bases such as 4-dodecylaniline. Finally, voltammetric data shows that lipophilic DMFc can also be extracted to the aqueous acidic phase to react homogeneously with oxygen.

1. Introduction

The interface between two immiscible electrolyte solutions (ITIES) is formed between two liquid solvents of a low mutual miscibility, such as water and 1,2-dichloroethane (DCE), each containing an electrolyte [1–4]. Electrochemical polarization of ITIES can be used to drive electron transfer and ion transfer reactions, but also to control adsorption phenomena. Hence, such interfaces have been considered as suitable models for investigating heterogeneous reactions occurring in biological systems, which are in many cases ion-coupled electron transfer reactions. Within aerobic living organisms, proton-coupled oxygen reduction consumes protons on one side of the biomembrane to generate a transmembrane proton gradient, leading to a transmembrane potential difference to drive the synthesis of adenosine triphosphate (ATP) for life activities [5]. Oxygen reduction at the ITIES has been so far studied by using various electron donors, decamethylferrocene (DMFc) [6–9], reduced flavin mononucleotide (FMN) [10], tetrachlorohydroquinone (CQH_2) [11] and fullerene monoanion (C_{60}^-) [12]. In the case of DMFc, it has been shown that oxygen reduction at the polarized water/DCE interface produces decamethylferrocenium ($DMFc^+$) and hydrogen peroxide (H_2O_2), on the basis of two-phase reactions [7] and *in situ* detection of H_2O_2 using scanning electrochemical microscopy [13]. The catalytic effect of various porphyrin compounds, such as cobalt tetraphenylporphyrin [9,14], cobalt porphine [15] and free base tetraphenylporphyrin [16] and electrodeposited platinum particles [8], on the oxygen reduction by DMFc at the water/DCE interface has also been investigated. Moreover, it has been found very recently that under anaerobic conditions DMFc could also reduce aqueous proton to produce hydrogen at the water/DCE interface [17].

This paper presents the electrochemical aspects, as well as some thermodynamic considerations of O_2 reduction by DMFc at the water/DCE interface. A reaction mechanism similar to an *EC* type reaction at the conventional electrode/solution interface is proposed, in which a proton transfer assisted by DMFc across the water/DCE interface is equivalent to the electrochemical step giving rise to a measurable current signal, and the following irreversible oxygen and/or proton reduction reactions represents the chemical step. The two steps are coupled at the interface, with protons supplied by the aqueous phase and electrons provided by DMFc in DCE. The standard redox potentials of O_2 reduction calculated on the basis of a thermodynamic cycle also suggests that the O_2 reduction is largely favored in DCE. The proposed *EC* type mechanism is also examined by further investigating the influence of a hydrophobic proton ionophore, 4-dodecylaniline (DA), on the oxygen reduction by DMFc at the water/DCE interface. Finally,

* Corresponding author. Fax: +41 21 6933667.
E-mail address: hubert.girault@epfl.ch (H.H. Girault).
[1] Present address: Institute of Microanalytical Systems, Department of Chemistry, Zhejiang University, 310058 Hangzhou, China.

1572-6657/$ - see front matter © 2009 Elsevier B.V. All rights reserved.
doi:10.1016/j.jelechem.2009.11.029

voltammetric data shows that lipophilic DMFc can be extracted to the aqueous acidic phase to react homogeneously with oxygen.

2. Experimental

2.1. Chemicals

All chemicals were used as received without further purification. All the aqueous solutions were prepared with ultra pure water (18.2 MΩ cm^{-1}). Decamethylferrocene (DMFc, 99%) was supplied by Alfa Aesar. Lithium tetrakis(pentafluorophenyl)borate diethyl etherate (LiTB) was provided by Sigma–Aldrich. Lithium chloride anhydrous (LiCl, ⩾99%), lithium sulfate (Li_2SO_4, >98.0%), sodium iodide (NaI, >99.5%), bis(triphenylphosphoranylidene)ammonium chloride (BACl, ⩾98%), 4-dodecylaniline (DA), tetramethylammonium chloride (TMACl, ⩾98%) and 1,2-dichloroethane (DCE, ⩾99.8%) were obtained from Fluka. Hydrochloric acid (HCl, 32%) and sulfuric acid (H_2SO_4, 5 M) were ordered from Merck. Tetramethylammonium tetrakis(pentafluorophenyl)borate (TMATB) and bis(triphenylphosphoranylidene)ammonium tetrakis(pentafluorophenyl)borate (BATB) were prepared as reported previously [18].

2.2. Electrochemical measurements

Electrochemical measurements at the water/DCE interface were performed in a four-electrode configuration on a commercial potentiostat (PGSTAT 30, Eco-Chemie, Netherlands) or on a custom-built system connected with a DS335 synthesized function generator (Stanford Research System). The electrochemical cell used was a three-compartment glass cell featuring a cylindrical vessel where the water/DCE interface with a geometric area of 1.53 cm^2 was formed. Two platinum counter electrodes were positioned in the aqueous and DCE phases, respectively, to supply the current flow. The external potential was applied between two reference electrodes, silver/silver chloride (Ag/AgCl) or silver/silver sulfate (Ag/Ag_2SO_4), which were connected to the aqueous and DCE phases respectively by means of a Luggin capillary. Electrolyte compositions are illustrated in Scheme 1. The potential was converted to the Galvani potential difference ($\Delta_o^w\phi$), based on cyclic voltammetric measurement of the reversible half-wave potential of the TEA^+ cation transfer (0.019 V) [19]. All the electrochemical measurements were performed at ambient temperature (23 ± 2 °C) with air-saturated solutions, unless specified otherwise.

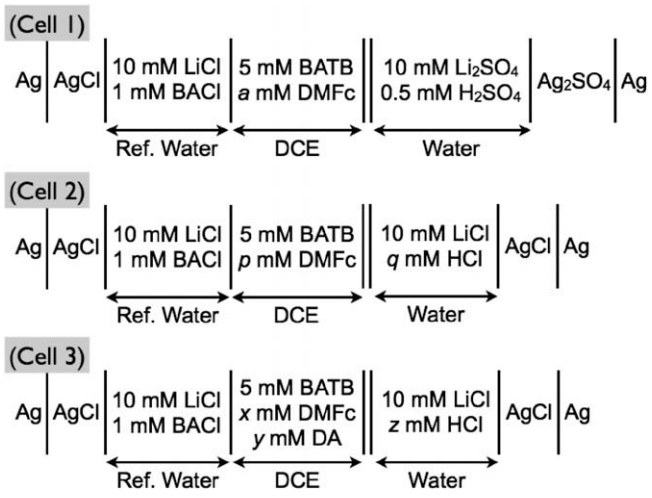

Scheme 1. Electrochemical cells employed.

2.3. Shake flask experiments with DA

The two-phase reactions including DA as a proton ionophore were performed in a small flask under stirring conditions. Firstly, the DCE solution (2 mL) containing 5 mM DMFc or 5 mM DMFc and 0.1 mM DA were added to the flask, followed by the addition of 2 mL of aqueous solution containing 10 mM HCl. The salts of the common ion (TMA^+), TMACl and TMATB, were added in the concentration of 5 mM and 50 mM to the aqueous and DCE phases, respectively, to fix the Galvani potential difference across the interface at 0.22 V according to the Nernst equation with TMA^+ standard ion transfer potential value of 0.16 V [19]. The two-phase system was first stirred for 20 min then left for phase separation and the aqueous and organic solutions were isolated from each other. The UV–visible absorption spectra of the organic solution and the aqueous solution treated by excess NaI were measured on an Ocean Optical CHEM2000 spectrophotometer using a quartz cuvette with a path length 10 mm.

3. Standard redox potentials of O_2/H^+ reduction reactions in DCE

3.1. General case

The redox potentials of various O_2 reduction reactions in water are well-known, whereas those in organic media are not. Hence, the standard redox potentials of various O_2 reduction reactions in DCE with respect to the Standard Hydrogen Electrode (SHE) are calculated on the basis of thermodynamic considerations. First, a general redox reaction is considered:

$$O(s) + ne^- \rightarrow R(s) \tag{1}$$

The standard redox potentials for the redox couple O/R in the aqueous phase and organic phase with respect to SHE are defined as [20]:

$$\left[E^{\ominus}_{O/R}\right]^{w}_{SHE} = \left[\left(\mu^{\ominus,w}_{O} - \mu^{\ominus,w}_{R}\right) - n\left(\mu^{\ominus,w}_{H^+} - \frac{1}{2}\mu^{\ominus}_{H_2}\right)\right]\Big/nF \tag{2}$$

$$\left[E^{\ominus}_{O/R}\right]^{o}_{SHE} = \left[\left(\mu^{\ominus,o}_{O} - \mu^{\ominus,o}_{R}\right) - n\left(\mu^{\ominus,w}_{H^+} - \frac{1}{2}\mu^{\ominus}_{H_2}\right)\right]\Big/nF \tag{3}$$

where $\mu^{\ominus,s}_{O}$ (s = o or w) and $\mu^{\ominus,s}_{R}$ (s = o or w) denote the standard chemical potentials of O and R, respectively. $\mu^{\ominus,w}_{H^+}$ and $\mu^{\ominus}_{H_2}$ represent the standard chemical potentials of proton in water and of hydrogen in gas phase. From Eqs. (2) and (3) we can get:

$$\begin{aligned}\left[E^{\ominus}_{O/R}\right]^{o}_{SHE} &= \left[E^{\ominus}_{O/R}\right]^{w}_{SHE} + \left[\left(\mu^{\ominus,o}_{O} - \mu^{\ominus,w}_{O}\right) - \left(\mu^{\ominus,o}_{R} - \mu^{\ominus,w}_{R}\right)\right]/nF \\ &= \left[E^{\ominus}_{O/R}\right]^{w}_{SHE} + \left(\Delta G^{\ominus,w\rightarrow o}_{tr,O} - \Delta G^{\ominus,w\rightarrow o}_{tr,R}\right)\Big/nF\end{aligned} \tag{4}$$

where $\Delta G^{\ominus,w\rightarrow o}_{tr,O}$ and $\Delta G^{\ominus,w\rightarrow o}_{tr,R}$ denote the standard Gibbs energy of transferring O and R from water to the organic phase, respectively. Eq. (4) tells that the work needed to reduce O to R in an organic phase is the sum of the work needed to reduce O to R in water plus that needed to transfer O from water to the organic phase and R from the organic to the aqueous phase. As reported previously, a series of redox potentials of ferrocene derivatives, such as $\left[E^{\ominus}_{DMFc^+/DMFc}\right]^{o}_{SHE}$ = 0.07 V in DCE, have been measured with respect to that of ferrocene [21]. Moreover, in the case of proton reduction reaction in DCE, its standard redox potential corresponds to the Gibbs transfer energy of proton across the water/DCE interface expressed in the voltage scale, that is 0.55 V [20].

3.2. $\left[E^{\ominus}_{O_2/O_2^-}\right]^{DCE}_{SHE}$

In the case of superoxide formation in a solution:

$$O_2(g) + e^- \rightarrow O_2^-(s) \quad (5)$$

The standard redox potentials for the redox couple O_2/O_2^- in the aqueous (s = w) and organic (s = o) phase with respect to SHE are:

$$\left[E^{\ominus}_{O_2/O_2^-}\right]^{w}_{SHE} = \left[\left(\mu^{\ominus}_{O_2} - \mu^{\ominus,w}_{O_2^-}\right) - \left(\mu^{\ominus,w}_{H^+} - \frac{1}{2}\mu^{\ominus}_{H_2}\right)\right]\Big/F \quad (6)$$

$$\left[E^{\ominus}_{O_2/O_2^-}\right]^{o}_{SHE} = \left[\left(\mu^{\ominus}_{O_2} - \mu^{\ominus,o}_{O_2^-}\right) - \left(\mu^{\ominus,w}_{H^+} - \frac{1}{2}\mu^{\ominus}_{H_2}\right)\right]\Big/F \quad (7)$$

where $\mu^{\ominus,s}_{O_2}$ (s = o or w) and $\mu^{\ominus,s}_{O_2^-}$ (s = o or w) denote the standard chemical potentials of O_2 and O_2^-, respectively. Arranging Eqs. (6) and (7) leads to:

$$\left[E_{O_2/O_2^-}\right]^{o}_{SHE} = \left[E^{\ominus}_{O_2/O_2^-}\right]^{w}_{SHE} + \left(\mu^{\ominus,w}_{O_2^-} - \mu^{\ominus,o}_{O_2^-}\right)\Big/F = \left[E^{\ominus}_{O_2/O_2^-}\right]^{w}_{SHE} - \Delta G^{\ominus,w\rightarrow o}_{tr,O_2^-}\Big/F \quad (8)$$

The Gibbs energy of transfer of O_2^- can be calculated knowing that the respective solubility of oxygen in water and 1,2-DCE is 2.5×10^{-4} mol dm^{-3} [22] and 1.39×10^{-3} mol dm^{-3} [23]. The standard Gibbs energy of transfer of molecular oxygen from water to DCE is then –4.25 kJ mol^{-1}. On the basis of the Born solvation model, we can calculate the Gibbs energy of transfer of the superoxide anion with

$$\Delta G^{\ominus,w\rightarrow o}_{tr,O_2^-} = \Delta G^{\ominus,w\rightarrow o}_{tr,O_2} + \frac{F^2}{8\pi\varepsilon_0 r_{O_2}}\left(\frac{1}{\varepsilon^o} - \frac{1}{\varepsilon^w}\right) \quad (9)$$

which yields assuming that the radius of molecular oxygen is equal to the bond length (120 pm) a value of 46.3 kJ mol^{-1}. With $\left[E^{\ominus}_{O_2/O_2^-}\right]^{w}_{SHE} = -0.330$ V, one obtain $\left[E^{\ominus}_{O_2/O_2^-}\right]^{DCE}_{SHE} \approx -0.81$ V in DCE.

3.3. $\left[E^{\ominus}_{O_2/H_2O_2}\right]^{DCE}_{SHE}$, $\left[E^{\ominus}_{O_2/H_2O}\right]^{DCE}_{SHE}$ and $\left[E^{\ominus}_{H_2O_2/H_2O}\right]^{DCE}_{SHE}$

In the case of a two-electron two-proton reduction of O_2 to H_2O_2 in a solution as expressed below:

$$O_2(g) + 2H^+(s) + 2e^- \rightarrow H_2O_2(s) \quad (10)$$

the standard redox potentials for the redox couple O_2/H_2O_2 in the aqueous (s = w) and organic (s = o) phase are:

$$\left[E^{\ominus}_{O_2/H_2O_2}\right]^{w}_{SHE} = \left[\left(\mu^{\ominus}_{O_2} + 2\mu^{\ominus,w}_{H^+} - \mu^{\ominus,w}_{H_2O_2}\right) - 2\left(\mu^{\ominus,w}_{H^+} - \frac{1}{2}\mu^{\ominus}_{H_2}\right)\right]\Big/2F \quad (11)$$

$$\left[E^{\ominus}_{O_2/H_2O_2}\right]^{o}_{SHE} = \left[\left(\mu^{\ominus}_{O_2} + 2\mu^{\ominus,o}_{H^+} - \mu^{\ominus,o}_{H_2O_2}\right) - 2\left(\mu^{\ominus,w}_{H^+} - \frac{1}{2}\mu^{\ominus}_{H_2}\right)\right]\Big/2F \quad (12)$$

Thus we get:

$$\left[E^{\ominus}_{O_2/H_2O_2}\right]^{o}_{SHE} = \left[E^{\ominus}_{O_2/H_2O_2}\right]^{w}_{SHE} + \left[\left(\mu^{\ominus,w}_{H_2O_2} - \mu^{\ominus,o}_{H_2O_2}\right) - 2\left(\mu^{\ominus,w}_{H^+} - \mu^{\ominus,o}_{H^+}\right)\right]\Big/2F = \left[E^{\ominus}_{O_2/H_2O_2}\right]^{w}_{SHE} - \left(\Delta G^{\ominus,w\rightarrow o}_{tr,H_2O_2} - 2\Delta G^{\ominus,w\rightarrow o}_{tr,H^+}\right)\Big/2F \quad (13)$$

The standard Gibbs energy of transfer of H_2O_2 across the water/DCE has been estimated to be close to that of H_2O being about 15.4 kJ mol^{-1} [24]. Therefore, with $\left[E^{\ominus}_{O_2/H_2O_2}\right]^{w}_{SHE} = 0.695$ V, one gets $\left[E^{\ominus}_{O_2/H_2O_2}\right]^{DCE}_{SHE} = 1.165$ V in DCE. Similarly, the standard redox potentials for the redox couples O_2/H_2O and H_2O_2/H_2O can be estimated to be $\left[E^{\ominus}_{O_2/H_2O}\right]^{DCE}_{SHE} = 1.738$ V and $\left[E^{\ominus}_{H_2O_2/H_2O}\right]^{DCE}_{SHE} = 2.312$ V, respectively.

The standard redox potentials of various O_2 reduction reactions are summarized in Table 1. It shows that O_2 reduction to O_2^- in DCE is more difficult than in an aqueous medium. Indeed, the reaction creates an anion that is less solvated than in water. In contrast, all the proton-coupled oxygen reduction reactions are favored in the organic phase, as they involve the elimination of charges.

4. Results and discussion

4.1. Proton transfer assisted by DMFc

Fig. 1a compares the cyclic voltammograms (CVs) in the absence (dotted line) and presence (solid lines) of 5 mM DMFc in DCE at a water/DCE interface under aerobic conditions. In the ab-

Table 1
Calculated standard redox potentials of proton reduction reaction and various O_2 reduction reactions.

Reaction	$[E^{\ominus}]^{w}_{SHE}$ (V)	$[E^{\ominus}]^{DCE}_{SHE}$ (V)
$H^+(s) + e^- \rightarrow 1/2H_2(g)$	0	0.55
$O_2(g) + e^- \rightarrow O_2^-(s)$	0.330	−0.81
$O_2(g) + 2H^+(s) + 2e^- \rightarrow H_2O_2(s)$	0.695	1.165
$O_2(g) + 4H^+(s) + 4e^- \rightarrow 2H_2O(s)$	1.229	1.738
$H_2O_2(s) + 2H^+(s) + 2e^- \rightarrow H_2O(s)$	1.763	2.312

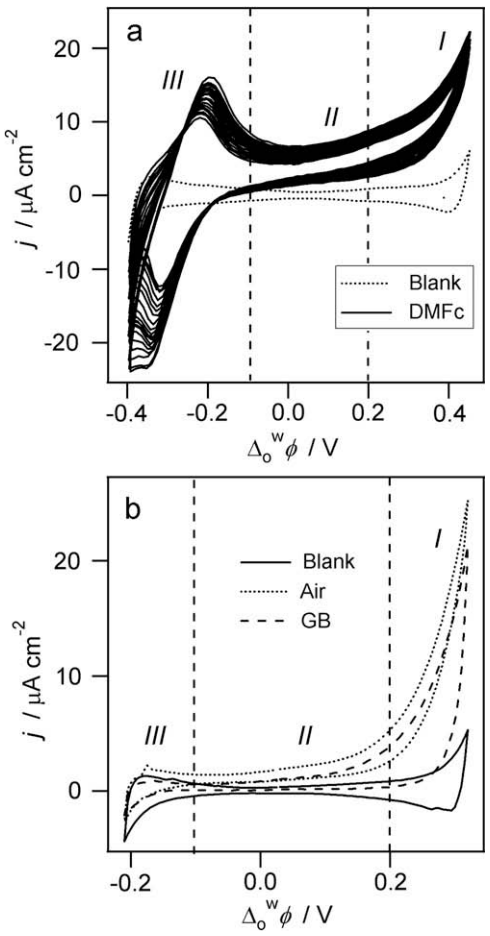

Fig. 1. (a) CVs obtained with Cell 1 in the absence ($a = 0$, dotted line) and presence (full lines, $a = 5$, 20 scans) of DMFc in DCE. The scan rate was 50 mV s^{-1}; (b) CVs obtained with Cell 2 in the absence ($p = 0$, $q = 100$, full line) and presence ($p = 5$, $q = 100$) of DMFc under aerobic (dotted line) and anaerobic (dashed line) conditions. The scan rate was 25 mV s^{-1}.

sence of DMFc, the CV presents a potential window from −0.4 V to 0.4 V limited by the transfer of SO_4^{-2} and H^+ from water to DCE on the negative and positive sides, respectively. In contrast, dissolving DMFc in DCE results in clearly three new features with respect to the blank one: (i) an irreversible positive current on the positive potential regime (*Signal I*), (ii) a positive current offset in the middle of the potential window (*Signal II*, that can be more clearly observed when using LiCl as the aqueous supporting electrolyte as shown in Figs. 1b, 2 and 5a, and that will be discussed later (Section 4.4), and (iii) a current wave in the negative potential range with a formal potential of $\Delta_o^w\phi = -0.26$ V (*Signal III*).

As shown in Fig. 1b, *Signal I* is independent of the presence of oxygen and of subsequent chemical reactions that were previously shown to yield H_2 under anaerobic conditions [17] and H_2O_2 in aerated solutions [7,13]. Indeed, the two curves are identical if the offset current of *Signal II* is subtracted. *Signal III* is associated with the transfer of $DMFc^+$ ion across the water/DCE interface produced during the reduction of oxygen. The Gibbs energy of transfer for $DMFc^+$ obtained from the mid-peak potential value is equal to 25.1 kJ mol^{-1}. Therefore, any Galvani potential difference more positive than –0.26 V is enough to keep $DMFc^+$ in the organic phase, which hinders its reaction with H_2O_2 in water. As reported previously a ferrocenium cation can be a Fenton reagent that reacts with H_2O_2 to form OH in water [25]. On the other hand, as shown in Fig. 1a upon successive cycles the current magnitude of *Signal I* does not change significantly whilst that of *Signal III* increases continuously. This fact indicates that when cycling the potential to the positive side where *Signal I* is observed, more and more $DMFc^+$ is produced by the subsequent chemical reactions.

The CVs compared in Fig. 1b therefore indicate that oxygen reduction is initiated by the assisted proton transfer by DMFc across the water/DCE interface:

$$DMFc_{(DCE)} + H^+_{(w)} \rightarrow DMFcH^+_{(DCE)} \quad (14)$$

This is supported by the pH dependence of *Signal I*, which shifts with the aqueous pH by approximately 60 mV/pH (Fig. 2), in accordance to the Nernst equation for an assisted ion transfer process occurring at the liquid/liquid interface. Essentially, this step corresponds to the protonation of DMFc but occurs heterogeneously in the present biphasic system, which gives rise to the experimentally observed electrical current, i.e. *Signal I*, with the four-electrode methodology at the liquid/liquid interface. Indeed, it is well-known that ferrocene compounds can be protonated either on the iron or on the cyclopentadienyl ring (Cp) or on both via an agostic position bridging iron and Cp [26]. In addition, the current magnitude decreases with increasing the aqueous pH, which is due to a lower concentration of proton in water at a higher pH and the proton diffusion starts to be a controlling factor. Also, at a higher pH the transfer of Li^+ will take place prior to that of the proton at the positive potential limit, since the formal ion transfer potentials of proton and lithium across the water/DCE interface are $\Delta_o^w\phi^{\ominus}_{H^+} = 0.549$ V and $\Delta_o^w\phi^{\ominus}_{Li^+} = 0.591$ V [19], respectively.

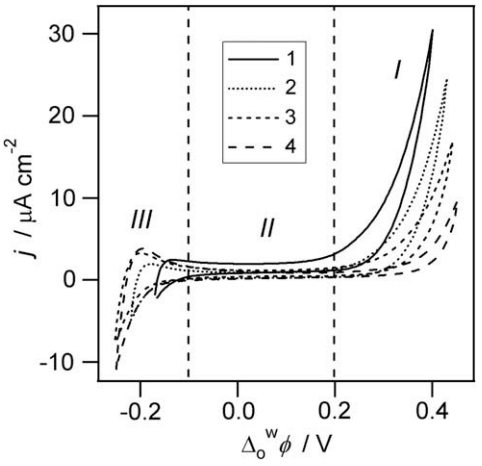

Fig. 2. CVs obtained with Cell 2 in the presence of DMFc in DCE ($p = 5$) at various pH. The pH was adjusted by adding HCl. The scan rate was 50 mV s^{-1}.

4.2. Oxygen reduction in aerobic conditions

In aerobic conditions, the generation of hydrogen peroxide (H_2O_2) has been verified by redox titration with sodium iodide [7] and scanning electrochemical microscopy [13]. Quantitative analysis of the reaction products after a two-phase reaction controlled by a common ion, as reported previously, the yield of H_2O_2 with respect to the amount of $DMFc^+$ is about 38% [7]. One of possible sources of the extra $DMFc^+$ might be the further reaction of produced H_2O_2 with DMFc as reported previously [27]. Indeed, H_2O_2 in DCE is an extremely strong oxidant with a standard redox potential of 2.312 V as calculated in the previous section. Therefore, from a viewpoint of H_2O_2 production a key advantage of the present biphasic system is to allow a very efficient collection of H_2O_2 by separating DMFc/$DMFc^+$ and H_2O_2 with a liquid junction between two phases, blocking effectively their further reactions [7]. Indeed, in the industrial Riedl–Pfleiderer process H_2O_2 formed by the auto-oxidation of 2-ethyl-9,10-dihydroxyanthracene in a hydrophobic solvent is also separated by an aqueous extraction [28]. Moreover, at the polarizable water/DCE interface the separation of $DMFc^+$ and H_2O_2 is reinforced by controlling the interfacial polarization either with an external voltage or with the partition of an ion.

O_2 reduction by ferrocene derivatives in organic media in the presence of an acid, such as carboxylic acids (trichloroacetic and trifluoroacetic acids) [29,30] and perchloric acid [27,31,32], has been studied for many years, although the reaction mechanism is yet unresolved. For example, the initial reaction step has been assigned to be the protonation on the Cp ring favoring the complexation of iron with O_2 [26,29,33–35] or that on the iron by the formation of Fe–H intermediate [34]. Preliminary density function theoretical computations support the hypothesis that triplet molecular oxygen O_2 approaches Fe–H directly via a delocalized triplet (diradical) transition state $[DMFc\cdots H\cdots OO\cdot]^+$ to yield a hydrogen peroxyl radical and H_2O_2 finally, which will be reported soon elsewhere.

Based on the experimental results and theoretical considerations, a reaction pathway illustrated in Scheme 2 is proposed for O_2/proton reduction by DMFc at the water/DCE interface. *APT* represents the assisted proton transfer across the water/DCE interface by DMFc described by Eq. (14) and *C* is the following O_2/proton reduction reaction. *C* can be simply considered as an irreversible chemical reaction responsible for the absence of backward proton transfer (proton transfer back to water from DCE). In this case, Scheme 2 is similar to an *EC* type reaction at the conventional electrode/solution interface. The *APT* step is equivalent to *E*,

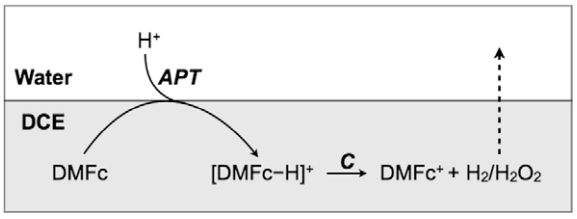

Scheme 2. Mechanism of O_2 and proton reduction by DMFc at the water/DCE interface.

which gives rise to the current signal experimentally observed. The following irreversible O_2/proton reduction reaction in DCE corresponds to the *C* step, which is a homogeneous reaction and then does not involve any charge flux across the water/DCE interface.

4.3. DA as a proton ionophore

A basic assumption in Scheme 2 is that the proton transfer step precedes the oxygen reduction. In order to prove it, 4-dodecylaniline (DA) that is a proton ionophore was included in DCE to investigate its influence on this reaction. DA is able to assist proton transfer from water to DCE at a lower Galvani potential difference instead at the limit of the potential window [36]. As shown in Fig. 3a, the proton transfer assisted by DA is presented by a reversible voltammetric wave with a formal Galvani potential difference of 0.22 V and a peak-to-peak separation of about 60 mV. A linear dependence on the square root of the scan rate of the peak current, as well as the shift of the formal potential with pH by about 60 mV/pH (not shown here) confirmed the voltammetric wave was resulted from the transfer of a singly-charged species, namely here proton. The dissociation constant of DA with proton was also estimated to be 6.4.

When both DMFc and DA are present, as shown in Fig. 3b, the anodic current due to the proton transfer assisted by DA from water to DCE was apparently enhanced and increased with increasing DMFc concentration, whereas the cathodic current due to the proton transfer back to DCE was obviously damped. This feature indicates that the presence of DMFc in DCE leads to the regeneration of DA from DAH^+ by an oxygen reduction process, and thus enhancing the assisted proton transfer current as illustrated in Scheme 3. In other words, DA functions as an effective phase transfer catalyst to bring protons from water to DCE for the protonation of DMFc.

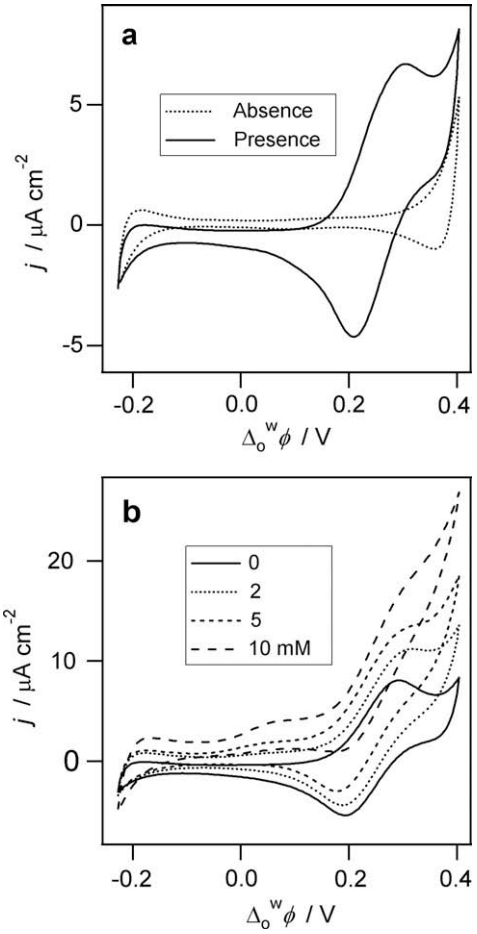

Fig. 3. (a) CVs obtained with Cell 3 in the absence ($x = 0$, $y = 0$, pH 2, dotted line) and presence ($x = 0$, $y = 0.05$, pH 2, full line) of DA in DCE; (b) CVs in the presence of DA and various concentrations of DMFc in DCE (Cell 3: $x = 0, 2, 5, 10$, $y = 0.05$, pH 2). The scan rate was 50 mV s^{-1}.

This system was also examined by a shake-flask experiment in which the Galvani potential difference across the interface was controlled at 0.22 V, where the facilitated proton transfer by DA from water to DCE occurs according to the CV shown in Fig. 3a. As demonstrated in Fig. 4a, the presence of both DA and DMFc in DCE resulted in a four times stronger absorption band at 779 nm due to $DMFc^+$ than that only DMFc in DCE, and the absorption band increased with increasing DA concentration (not shown here). Also, titration of the aqueous solutions by excess NaI suggested that the amount of H_2O_2 produced in the presence of both DA and DMFc is much higher that only DMFc in DCE, as shown by the two absorption bands of I_3^- at 286 nm and 352 nm (Fig. 4b). These shake-flask experiments therefore corroborate the electrochemical data, and an important point inferred is that the proton transfer from water to DCE precedes the oxygen reduction by DMFc in DCE, proving the reaction mechanism proposed in Scheme 3. These experimental data are indeed in agreement with a recent experimental work showing that O_2 reduction by DMFc could proceed in an aprotic solvent in the presence of imidazolium cation, which contains only an acidic C2-proton [37].

4.4. DMFc partition and Signal II

One remaining issue associated with the present experimental system is the current offset in the middle of the potential window, i.e. *Signal II* in Fig. 1, which is almost constant and potential-independent (Figs. 2 and 5a). The current offset starts from the electrochemical wave of $DMFc^+$ from water to DCE, and its positive sign indicates that it corresponds to a positive charge transfer from the aqueous to organic phase. Moreover, the magnitude of this current offset linearly increases with increasing DMFc concentration in DCE (Fig. 5b).

To unravel its origin, a biphasic test without electrochemical control was first performed, in which a concentrated DCE solution containing 50 mM DMFc was put in contact with an acidic aqueous solution (pH 2 adjusted by HCl) in a volume ratio of 5:2 (v/v, DCE/Water). As could be observed, the aqueous phase turned greener with time (Fig. 6). UV–visible spectroscopic measurement (Fig. 7) revealed the formation of $DMFc^+$ in water phase with a characteristic absorption band at 779 nm, which grows continuously with

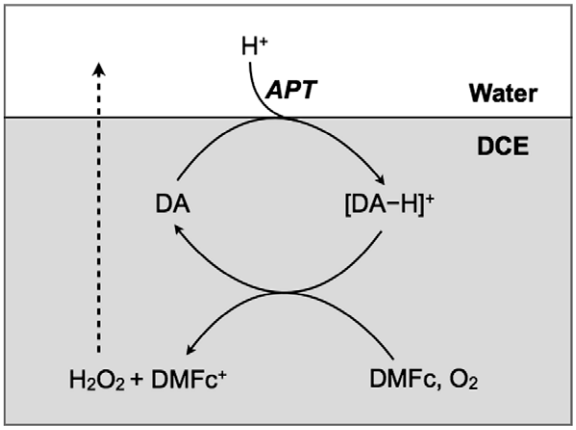

Scheme 3. Mechanism of O_2 reduction by DMFc using DA as a phase transfer catalyst.

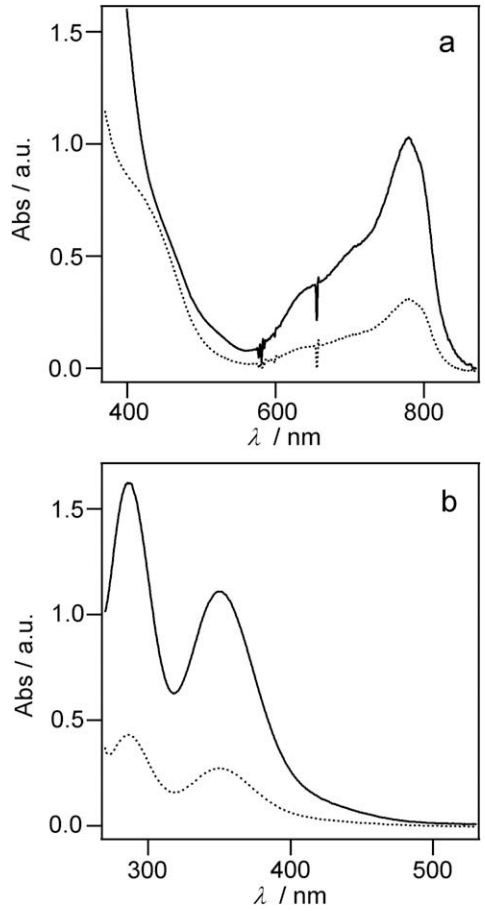

Fig. 4. UV–visible spectra of DCE solution (a) and aqueous solution treated by excess NaI (b) after biphasic stirring 20 min using TMA^+ as a common ion (5 mM TMACl in water and 50 mM TMATB in DCE). The aqueous phase contained 10 mM HCl in all three cases. The DCE phase contained: 5 mM DMFc (dotted), 0.1 mM DA and 5 mM DMFc (full).

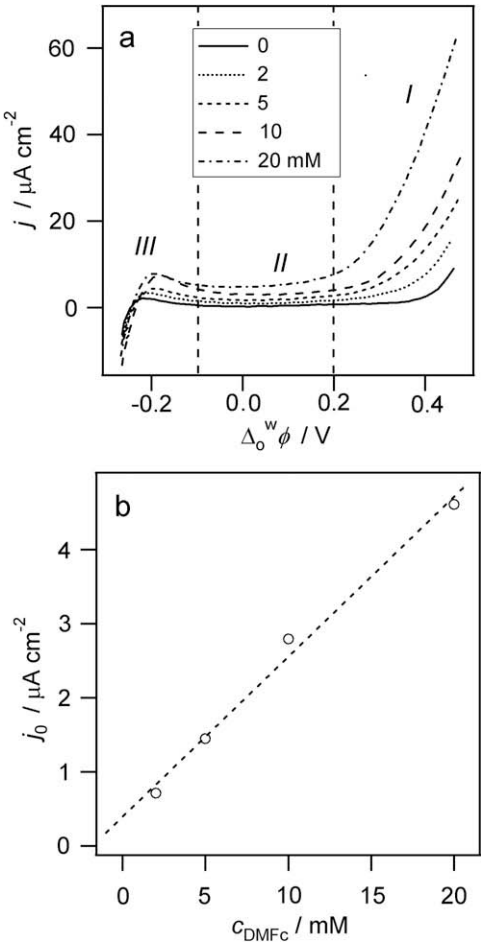

Fig. 5. (a) Linear scan voltammogram obtained with Cell 2 at various concentrations of DMFc in DCE (p = 0, 2, 5, 10 and 20, pH 2). The scan started from the left at a rate of 20 mV s^{-1}; (b) Dependence of the electrical current at 0 V in (a) on the DMFc concentration.

time. Because the water/DCE interface is not polarized and the DCE phase is ion-free, the transfer of ions including protons from water to DCE can only occur in the presence of a very lipophilic counterion. The production of $DMFc^+$ in water therefore most probably proceeds by the partition of DMFc from DCE to water followed by oxidation with O_2 on the aqueous side of the interface, as illustrated in Scheme 4. Furthermore, the transfer of thus formed $DMFc^+$ from water to DCE, that is the *IT* step in Scheme 4, gives rise to the positive current offset observed in the CV under the electrochemical polarization. Indeed, previous investigations have found that the electron transfer between ferrocene and hexacyanoferrate(III) at the liquid/liquid interface occurs by the same route, partitioning of ferrocene to water and reaction with hexacyanoferrate(III) homogeneously on the aqueous side of the interface [38]. Considering that oxygen is more soluble in DCE than in water, oxygen reduction by DMFc on the aqueous side of the interface is likely to be accompanied by oxygen transfer at the water/DCE interface and by transfer from the surrounding air atmosphere [39,40].

Considering Scheme 4, the current offset is the steady state diffusion current due to $DMFc^+$ transfer back from water, following the partition of DMFc from the organic phase and H_2O_2 production on the aqueous phase of the interface. Thus, if one assumes the aqueous reaction between DMFc and O_2/H^+ to be fast, the production of $DMFc^+$ in water is controlled by the rate of arrival of DMFc from the bulk organic phase to the interface. As a matter of fact, the steady state diffusion current increases monotonically with the DMFc concentration, indicating that the reaction is not limited by oxygen and proton supply. Accordingly, the sustained production

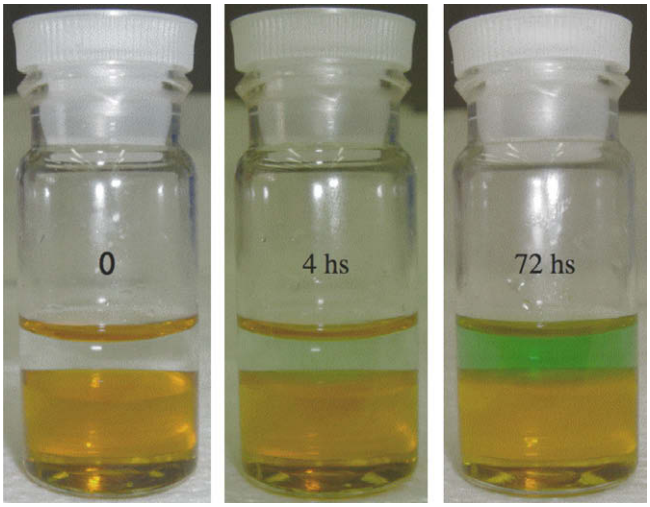

Fig. 6. Illustration of a biphasic test without electrochemical control: a 5 mL of DCE solution containing 50 mM DMFc was put in contact with a 2 mL aqueous solution (pH 2, adjusted by HCl).

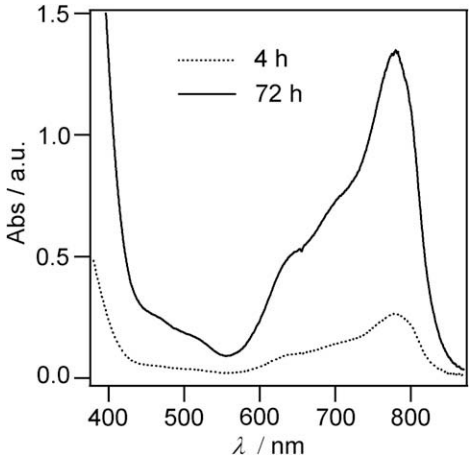

Fig. 7. UV–visible spectra of the aqueous solution after the biphasic test shown in Fig. 6 (the top solution in the right flask).

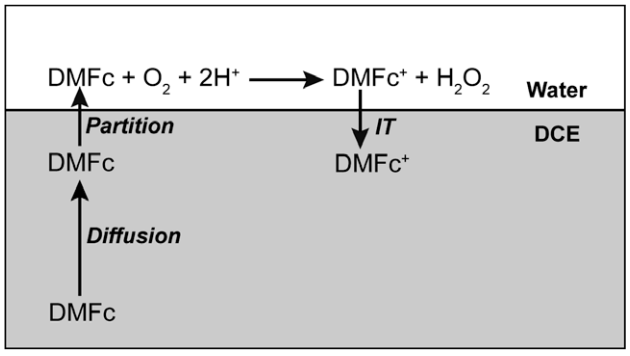

Scheme 4. Mechanism of partition of DMFc and reaction with O_2 in water.

of $DMFc^+$ on the aqueous side of the interface can be envisaged as a diffusion-limited reaction, as follows:

$$j = -D^{o}_{DMFc}\frac{c^{o,\infty}_{DMFc} - c^{o,0}_{DMFc}}{\delta} \approx -D^{o}_{DMFc}\frac{c^{o,\infty}_{DMFc}}{\delta} \quad (15)$$

Naturally, $DMFc^+$ will be afterwards transferred across the interface, giving rise to the aforementioned steady-state current.

5. Conclusions

O_2 reduction by DMFc at the polarized water/DCE interface proceeds as a proton-coupled electron transfer process, with protons supplied by the aqueous phase and electrons provided by DMFc in DCE. The reaction can be equivalent to an *EC* type mechanism at the conventional solid/solution interface, with the assisted proton transfer by DMFc across the water/DCE interface equivalent to the *E* step. The following irreversible oxygen reduction reaction and/or proton reduction reaction involving protonated DMFc, $DMFcH^+$, in DCE represent the chemical step.

Acknowledgements

This work was supported by Ecole Polytechnique Fédérale de Lausanne (EPFL), the Swiss Natural Science Foundation (FNRS 200020-116588) and the European Cooperation in the field of Scientific and Technological Research (COST Action, D36/007/06). I.H. also gratefully acknowledges the Scientific and Technological Research Council of Turkey (TUBITAK) under the 2212-PhD Scholarship Programme. Z.S. is also grateful to the Grant Agency of the Czech Republic (Grant No. 203/07/1257).

References

[1] J. Koryta, Electrochim. Acta 24 (1979) 293.
[2] Z. Samec, Chem. Rev. 88 (1988) 617.
[3] H.H. Girault, in: R.E. White, B.E. Conway, J.O.M. Bockris (Eds.), Modern Aspects of Electrochemistry, vol. 25, Plenum, New York, 1993, p. 1.
[4] H.H. Girault, D.J. Schifferin, in: A.J. Bard (Ed.), Electroanalytical Chemistry, vol. 15, Dekker, New York, 1989, p. 1.
[5] R. Boulatov, in: J.H. Zagal, F. Bedioui, J.-P. Dodelet (Eds.), N_4-Macrocyclic Metal Complexes, Springer, New York, 2006, p. 1.
[6] V.J. Cunnane, G. Geblewicz, D.J. Schiffrin, Electrochim. Acta 40 (1995) 3005.
[7] B. Su, R.P. Nia, F. Li, M. Hojeij, M. Prudent, C. Corminboeuf, Z. Samec, H.H. Girault, Angew. Chem., Int. Ed. 47 (2008) 4675.
[8] A. Trojanek, J. Langmaier, Z. Samec, Electrochem. Commun. 8 (2006) 475.
[9] A. Trojanek, V. Marecek, H. Janchenova, Z. Samec, Electrochem. Commun. 9 (2007) 2185.
[10] M. Suzuki, M. Matsui, S. Kihara, J. Electroanal. Chem. 438 (1997) 147.
[11] H. Ohde, K. Maeda, Y. Yoshida, S. Kihara, J. Electroanal. Chem. 483 (2000) 108.
[12] P. Liljeroth, B.M. Quinn, K. Kontturi, Langmuir 19 (2003) 5121.
[13] F. Li, B. Su, F. Cortes-Salazar, R. Partovi-Nia, H.H. Girault, Electrochem. Commun. 11 (2009) 473.
[14] R. Partovi-Nia, B. Su, F. Li, C.P. Gros, J.M. Barbe, Z. Samec, H.H. Girault, Chem. Eur. J. 15 (2009) 2335.
[15] I. Hatay, B. Su, F. Li, M.A. Mendez, T. Khoury, C.P. Gros, J.-M. Barbe, M. Ersoz, Z. Samec, H.H. Girault, J. Am. Chem. Soc. 131 (2009) 13453.
[16] A. Trojanek, J. Langmaier, B. Su, H.H. Girault, Z. Samec, Electrochem. Commun. 11 (2009) 1940.
[17] I. Hatay, B. Su, F. Li, R. Partovi-Nia, H. Vrubel, X. Hu, M. Ersoz, H.H. Girault, Angew. Chem., Int. Ed. 48 (2009) 5139.
[18] B. Su, J.-P. Abid, D.J. Fermin, H.H. Girault, H. Hoffmannova, P. Krtil, Z. Samec, J. Am. Chem. Soc. 126 (2004) 915.
[19] T. Wandlowski, V. Marecek, Z. Samec, Electrochim. Acta 35 (1990) 1173.
[20] H.H. Girault, Analytical and Physical Electrochemistry, EPFL Press, Lausanne, 2004.
[21] N. Eugster, D.J. Fermin, H.H. Girault, J. Phys. Chem. B 106 (2002) 3428.
[22] D. Plectcher, S. Sotiropoulos, J. Chem. Soc., Faraday Trans. 91 (1995) 457.
[23] P. Luehring, A. Schumpe, J. Chem. Eng. Data 34 (1989) 250.
[24] Z. Samec, Rev. Polaro. Kyoto. 55 (2009) 75.
[25] Z. Brusova, K. Stulik, V. Marecek, J. Electroanal. Chem. 563 (2004) 277.
[26] M.L. McKee, J. Am. Chem. Soc. 115 (1993) 2818.
[27] S. Fukuzumi, S. Mochizuki, T. Tanaka, Inorg. Chem. 28 (1989) 2459.
[28] W. Eul, A. Moeller, N. Steiner, in: A. Seidel (Ed.), Kirk-Othmer Encyclopedia of Chemical Technology, fifth ed., vol. 14, John Wiley & Sons, Inc.. Hoboken, 2005, p. 35.
[29] T.E. Bitterwolf, A.C. Ling, J. Organometal. Chem. 40 (1972) C29.
[30] R. Prins, A.G.T.G. Kortbeek, J. Organometal. Chem. 33 (1971) C33.
[31] S. Fukuzumi, S. Mochizuki, T. Tanaka, Chem. Lett. (1989) 27.
[32] S. Fukuzumi, K. Okamoto, C.P. Gros, R. Guilard, J. Am. Chem. Soc. 126 (2004) 10441.
[33] M. Buehl, S. Grigoleit, Organometallics 24 (2005) 1516.
[34] V.M. Fomin, A.E. Shirokov, N.G. Polyakova, P.A. Smirnov, Russ. J. Gen. Chem. 77 (2007) 652.
[35] M. Meot-Ner, J. Am. Chem. Soc. 111 (1989) 2830.
[36] M. Velazquez-Manzanares, D.J. Schiffrin, Electrochim. Acta 49 (2004) 4651.
[37] D.S. Choi, D.H. Kim, U.S. Shin, R.R. Deshmukh, S.-g. Lee, C.E. Song, Chem. Commun. (2007) 3467.
[38] H. Hotta, S. Ichikawa, T. Sugihara, T. Osakai, J. Phys. Chem. B 107 (2003) 9717.
[39] A.L. Barker, J.V. Macpherson, C.J. Slevin, P.R. Unwin, J. Phys. Chem. B 102 (1998) 1586.
[40] C.J. Slevin, S. Ryley, D.J. Walton, P.R. Unwin, Langmuir 14 (1998) 5331.